Measurement of heterogeneous uptake of NO2 on inorganic particles, sea water and urban grime

C. Yu, Z. Wang, Q. Ma, L. Xue, C. George

Measurement of heterogeneous uptake of NO_2 on inorganic particles, sea water and urban grime

Chuan Yu [1,2], Zhe Wang [2,3]*, Qingxin Ma [4], Likun Xue [1], Christian George [5], and Tao Wang [2,*]

[1] Environment Research Institute, Shandong University, Ji'nan, Shandong, China; yuchuan_sdu@hotmail.com (C.Y.); xuelikun@sdu.edu.cn (L.X.)
[2] Department of Civil and Environmental Engineering, The Hong Kong Polytechnic University, Hong Kong, China; z.wang@ust.hk (Z.W.); cetwang@polyu.edu.hk (T.W.)
[3] Division of Environment and Sustainability, The Hong Kong University of Science and Technology
[4] Research Center for Eco-Environmental Sciences, Chinese Academy of Sciences, Beijing 100085, China; qxma@rcees.ac.cn
[5] Univ Lyon, Université Claude Bernard Lyon 1, CNRS, IRCELYON, F-69626, Villeurbanne, France; christian.george@ircelyon.univ-lyon1.fr
* Correspondence: z.wang@ust.hk (Z.W.); cetwang@polyu.edu.hk (T.W.)

Abstract: Heterogeneous reactions of NO_2 on different surfaces play an important role in atmospheric NO_x removal and HONO formation, having profound impacts on photochemistry in polluted urban areas. Previous studies have suggested that the NO_2 uptake on the ground or aerosol surfaces could be a dominant source for elevated HONO during daytime. However, the uptake behavior of NO_2 varies with different surfaces, and different uptake coefficients were used or derived in different studies. To obtain a more holistic picture of heterogeneous NO_2 uptake on different surfaces, a series of laboratory experiments using different flow tube reactors was conducted, and the NO_2 uptake coefficient (γ) were determined on inorganic particles, sea water and urban grime. The results showed that heterogeneous reactions on those surfaces were generally weak in dark condition, with the measured γ varied from $<10^{-8}$ to 3.2×10^{-7} under different humidity. A photo-enhanced uptake of NO_2 on urban grime were observed, with obvious formation of HONO and NO from the heterogeneous reaction. The photo-enhanced γ was measured to be 1.9×10^{-6} to at 5% RH and 5.8×10^{-6} at 70% RH on urban grime, showing a positive RH dependence for both NO_2 uptake and HONO formation. The results demonstrate an important role of urban grime in the daytime NO_2-to-HONO conversion, and could be helpful to explain the unknown daytime HONO source in the polluted urban area.

Keywords: NO_2 uptake; HONO source; heterogeneous uptake coefficient; urban grime

1. Introduction

The heterogeneous reaction of NO_2 on different surfaces acts as an important NO_x sink and also a major source of nitrous acid (HONO), thus affecting the atmospheric nitrogen cycle and photochemistry [1]. Several previous laboratory studies have measured the heterogeneous uptake of NO_2 on inorganic particles, such as SiO_2 [2,3], Al_2O_3 [4,5] and $CaCO_3$ [6], but the reactivity of NO_2 on inorganic particles (expressed as an uptake coefficient, γ) is usually low (γ lies in the range from $<10^{-8}$ to 10^{-7}). Enhanced reactivity of NO_2 was found when irradiation was involved in the heterogeneous process. For example, the photo-enhanced uptake of NO_2 have been found on polycyclic aromatic hydrocarbons (PAHs) [7-10], humic acid (HA) [11-13], soot [14,15] and mineral dust [3,16]. The photo-enhanced γ is usually within 10^{-7}~10^{-6}, larger than those on inorganic particles at dark by one or two orders of magnitude. Moreover, enhanced HONO formation was also often observed together with the photo-enhanced uptake of NO_2 [7-10,11,12,14].

HONO could act as an important source of hydroxyl radical (OH) through photolysis and therefore plays an important role in the oxidation capacity of the atmosphere. Gas-phase reaction of NO and OH and nocturnal heterogeneous reaction of NO_2 on surfaces have been recognized as the major HONO sources at daytime and nighttime, respectively (e.g. [1,17]). A recent study at a coastal site in Hong Kong has observed that the NO_2-to-HONO conversion rate in the air masses passing

over the sea was almost 3 times larger than that in the land air masses, suggesting that the air-sea interaction at the sea surface could be a source of HONO [18]. Some studies also revealed significant unknown daytime sources of HONO that cannot be explained by the traditional gas-phase oxidation process [19], and several potential daytime sources or mechanism have been proposed, including traffic emissions [20,21], photo-enhanced heterogeneous reaction of NO_2 on surfaces containing humic acid, PAHs and soot [7,11,14], photolysis of nitrate [22-25] and nitric acid [26,27], etc.

In urban area, particles and urban surfaces provide a large surface area for the heterogeneous reactions of trace gases. A model study predicted that in highly urbanized area, the surface area provided by the ground surface could be 3 times larger than the atmospheric aerosol surface, and could be more important for heterogeneous reaction of NO_2 in urban area [28]. Furthermore, urban surfaces such as buildings and roads are usually covered with a film of a complex mixture of organic and inorganic materials, which are called urban grimes [29-32]. A recent study has reported a photo-enhanced uptake of NO_2 and HONO production on real urban grime and , with γ of $(1.1\text{-}5.8)\times10^{-6}$ at RH range of 0% - 90% [33]. As the physical and chemical properties of urban grime vary with locations [29-32], the heterogeneous behavior of NO_2 on more urban grime under different conditions should be investigated [33], in order to better quantify the roles of heterogeneous reactions on urban grime in HONO production and urban air quality, especially for highly urbanized environment with more NO_x emission and building surfaces.

In this study, to enrich the present understanding of NO_2 heterogeneous reactivity and to explore the unknown source of HONO, we conducted a series of laboratory experiments on different surfaces. We measured the heterogeneous uptake of NO_2 on SiO_2, Al_2O_3, $CaCO_3$, NaCl and $(NH_4)_2SO_4$ particle surface by a coated-wall flow tube, and on NaCl solution and sea water surface using a wetted-wall flow tube. We also investigate the NO_2 heterogeneous process and HONO production on urban grimes collected in Hong Kong with high building density and compact urban setting.

2. Experiments

2.1 Coated wall flow tube

A horizontal cylindrical coated-wall flow tube was used to study the NO_2 uptake on solid particles (Figure 1a), and similar apparatus and techniques have been employed and described in many studies [34-36]. The flow tube was made of quartz glass with a length of 34 cm and an inner diameter of 1.6 cm. Powder sample was dissolved in 20.0 mL of deionized water (for MgO, SiO_2, Al_2O_3, and $CaCO_3$) or ethanol (for NaCl and $(NH_4)_2SO_4$) and then was dripped into a quartz tube (20.0 cm length, 1.1 cm i.d.) and dried for 12 hours in an oven at 373 K. SiO_2 (99.9%), Al_2O_3 (99.9%), $CaCO_3$ (99.9%), NaCl (99.9%), $(NH_4)_2SO_4$ (99.9%) and ethanol (99.9%) were purchased from Sigma-Aldrich. The specific surface area was measured by nitrogen Brunauer-Emmett-Teller (BET) physisorption (Quantachrome Autosorb-1-C) and was 135.6 $m^2\ g^{-1}$ for MgO, 4.2 $m^2\ g^{-1}$ for SiO_2, 12 $m^2\ g^{-1}$ for Al_2O_3, 0.6 $m^2\ g^{-1}$ for $CaCO_3$, 0.22 $m^2\ g^{-1}$ for NaCl, and 0.16 $m^2\ g^{-1}$ for $(NH_4)_2SO_4$, respectively. Experiments were carried out at 295 K by thermostatic circulation of water through the outer jacket of the flow tube and the flow tube was covered to shield from the light during the experiments. Zero air was introduced in the flow tube as carrier gas at a flow rate of 0.9 L min^{-1}, ensuring a laminar regime. The RH of the carrier gas was adjusted by a water bubbler. NO_2 (10 ppmv in N_2; 99%; Arkonic) was introduced in the flow tube via a movable injector (with an inner diameter of 0.3 cm) and the NO_2 concentration in the total flow was 100 ppbv. At the exit of the flow tube, NO concentration, NO_2 concentration and RH were measured.

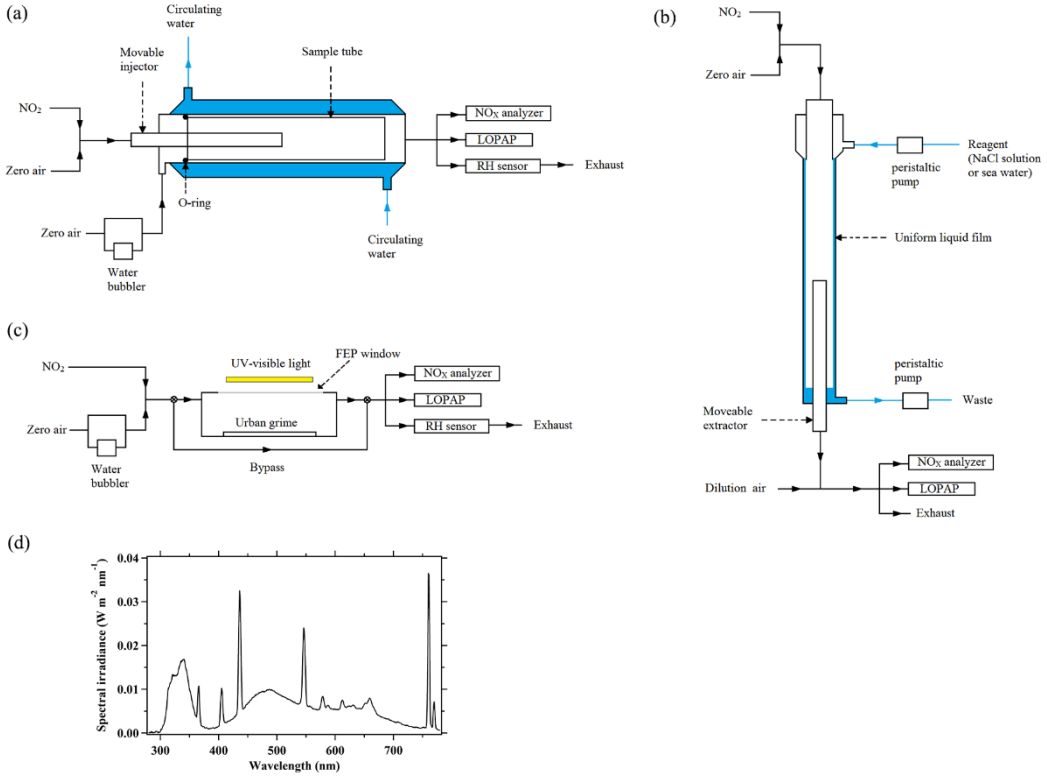

Figure 1. Schematic diagrams of (**a**) the coated wall flow tube system, (**b**) the wetted wall flow tube system, and (**c**) the Teflon box reactor system. (**d**) Spectral irradiance of the UV-visible light measured in the Teflon reactor.

2.2 Wetted wall flow tube experiments

A wetted wall flow tube system was developed following the design of Behnke et al. [37] and Gutzwiller et al. [38]. The vertical flow tube was made of glass with a length of 120 cm and an inner diameter of 0.8 cm (Figure 1b). Experiments were carried out at 295 K by thermostatic circulation of water through the outer jacket of the flow tube and the flow tube was covered to shield from the light during the experiments. 3.5 wt% NaCl solution was prepared by NaCl (99.9%; Sigma-Aldrich) and deionized water. Sea water was collected at Hok Tsui, Hong Kong in July 30, 2017. Reagent (NaCl solution or sea water) was pumped in at the top of the wetted wall flow tube by a peristaltic pump at a flow rate of 3 ml min^{-1}. Using an annular reservoir dispenser system, the reagent flowed down uniformly on the inner wall of the flow tube and was pumped out at the bottom of the flow tube. A mixture of NO_2 and zero air (NO_2 concentration of 300 ppbv) was introduced in the flow tube at a flow rate of 400 mL min^{-1}, ensuring a laminar regime. Then after contact with the reagent, the gas exited from a Teflon moveable extractor and diluted by dry zero air at a flow rate of 1700 mL min^{-1}. NO, NO_2 and HONO concentrations in the outflow were monitored.

2.3 Teflon box reactor experiments

A PFA box reactor (inner size of 25×15×5 cm, with a 22.5×12.5 cm FEP window on the top) was used to study the uptake coefficient of NO_2 on urban grime (Figure 1c). The box was covered to shield from the light in the dark experiments or illuminated by an 18 W UV-visible light (Arcadia Products plc.) in the irradiation experiments. A fan outside the reactor was used for cooling the UV-visible light, and the experiments were performed at room temperature around 295K. Before the experiment, the spectral irradiance inside the reactor was measured by a Spectro-Radiometer (specbos 1211UV, JETI Technische Instrumente GmbH.), as shown in figure 1d , and a total irradiance of 2.1 W m^{-2} was measured in the wavelength range of 280–780 nm. The photolysis frequency of NO_2, j_{NO2}, was

measured to be 1.8×10^{-4} s^{-1} by a j_{NO2} filter radiometer (Meteorologie Consult). Urban grime samples were collected by placing 20×10 cm glass plates underneath a building overhang at the Hong Kong Polytechnic University from August 21 to September 3, 2017, and the weight of each sample is about 0.01g. A glass plate with urban grime was placed in the box reactor to investigate NO_2 uptake on urban grime or a clean glass plate was placed in the blank experiment. NO_2 and zero air were introduced in the box reactor and the total flow rate was changed from 3 to 5 LPM resulting in resistant time from 37.5 to 22.5 s. The initial NO_2 concentration was 57 ppbv. A water bubbler was used to humidify the zero air and adjust the RH. Photolysis experiments of urban grime was also tested and the experiment setup and conditions were the same as the urban grime experiments except that only zero air was introduced into the reactor. The NO, NO_2 and HONO concentrations and RH were measured at the exit of the box reactor.

2.4 Instrumentation

At the exits of the reactors, NO and NO_2 concentrations were measured by a chemiluminescence analyzer with a photolytic converter (Thermo, 42i), HONO concentration was measured by a long-path absorption photometer (QUMA, LOPAP) [39,40] and the relative humidity (RH) was measured by a RH sensor (Omega, RH-USB). Reacted and fresh urban grime samples were sonicated in 50 mL Milli-Q water to extract the inorganic compositions and the concentrations of the inorganic ions in the urban grime samples were measured by an ion chromatograph (Dionex, ICS 1000).

2.5 Calculation of uptake coefficient

The reaction of NO_2 on different surfaces was assumed to be a pseudo-first-order reaction and the first-order rate constant (k_{obs}) can be calculated by:

$$k_{obs}=\ln\left(\frac{(NO_2)_0}{(NO_2)_t}\right)/t \ , \quad (1)$$

where $(NO_2)_0$ is the initial NO_2 concentration and $(NO_2)_t$ is the NO_2 concentration after the reaction time t with the surface.

The geometric uptake coefficient γ_{geo} of the flow tube experiments can be calculated by:

$$\gamma_{geo}=\frac{2\, r_{tube}\, k_{obs}}{c}, \quad (2)$$

where r_{tube} is the radius of the flow tube and c is the average molecular velocity of NO_2.

The Cooney–Kim–Davis (CKD) method was used to correct the gas phase diffusion limitations in the calculation of the geometric uptake coefficient γ [41,42]. And for the coated wall flow tube experiments, the true uptake coefficient (γ_{BET}) on particles was calculated by Eq. (3) [36,43].

$$\gamma_{BET}=\frac{S_{geo}}{S_{BET}}\times slope, \quad (3)$$

where S_{geo} is the inner wall surface area of the quartz tube, S_{BET} is the particle sample surface area and *slope* is the slope of the plot of the geometric uptake coefficient γ versus the sample mass in the linear regime.

The geometric uptake coefficient γ_{geo} in the urban grime experiments was calculated by:

$$\gamma_{geo}=\frac{4\, V_{box}\,(k_{obs\_grime}-k_{obs\_glass})}{S_{glass}\, c}, \quad (4)$$

where k_{obs_grime} and k_{obs_glass} are the first-order rate constants measured with the urban grime sample or with a clean glass plate, the V_{box} is the volume of the box reactor, S_{glass} is the surface area of the glass plate and c is the average molecular velocity of NO_2.

Yields of NOHO and NO are calculated by:

$$\text{Yield}=\frac{(\Delta\text{Product})_{grime}-(\Delta\text{Product})_{glass}}{(\Delta NO_2)_{grime}-(\Delta NO_2)_{glass}}, \quad (5)$$

where $(\Delta Product)_{grime}$ and $(\Delta Product)_{glass}$ are the HONO or NO concentrations produced from NO_2 reactions on urban grime or on a clean glass plate; $(\Delta NO_2)_{grime}$ and $(\Delta NO_2)_{glass}$ are the NO_2 consumed on urban grime or on a clean glass plate.

The flux of HONO production from the urban grime surface was calculated by:

$$Flux = \frac{((\Delta HONO)_{grime} - (\Delta HONO)_{glass}) fP}{RTAS_{glass}}, \quad (6)$$

$(\Delta HONO)_{grime}$ and $(\Delta HONO)_{glass}$ are the HONO concentration produced from NO_2 uptake on urban grime of on a clean glass plate; f is the total flow introduced into the box reactor; P is ambient pressure; R is molar gas constant, taken as 8.314 J mol^{-1} K^{-1}; T is ambient temperature; A is the Avogadro's constant; and S_{glass} is the surface area of the glass plate.

3. Results and Discussion

3.1. NO_2 uptake on inorganic particles

Figure 2 shows the typical uptake experiment of NO_2 on inorganic particles, and the measured true uptake coefficient γ_{BET} on all of the tested inorganic particles are less than 3.2×10^{-7}, as summarized in Table 1. On each type of particles, experiments were conducted at least at two RH conditions. The results indicate that the heterogeneous uptake of NO_2 on these inorganic particles are generally weak, even at high humidity. In Table 1, previous results from other studies on inorganic particles are also summarized and compared [2-6,44,45]. The pressure and humidity conditions of coated wall flow tube are much closer to ambient conditions than some techniques such as Knudsen cell reactor used in the previous studies. The results measured in the present study are slightly higher than previous studies on the mineral particle surfaces [2-6], except for NaCl [44,45]. The γ_{BET} on NaCl was much smaller than the values measured in two previous studies using aerosol flow tube ($<10^{-4}$ and 3.7×10^{-4}-1×10^{-3}) [44,45], and the discrepancy could be partially due to the different experiment techniques and also the much higher NO_2 concentration (ppm level) in the previous studies. Future experiments under atmospheric condition are still needed to measure the γ of NO_2 on mixed real ambient aerosols.

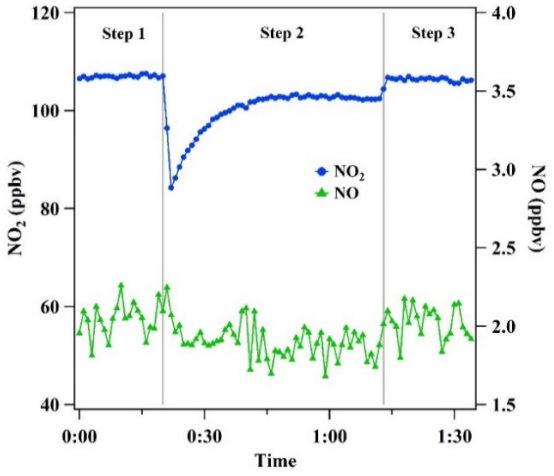

Figure 2. NO_2 uptake on $CaCO_3$. Blue circles and green triangles represent the NO_2, and NO concentrations at the exit of the reactor. The grey vertical lines indicate the experimental steps. Step 1: reactor bypass; step 2: $CaCO_3$ exposed to NO_2 in the dark; step 3: reactor bypass line.

Table 1. Summary of the NO_2 uptake coefficient on different surfaces.

Surface	Irradiation	RH (%)	γ	γ in previous studies	References
SiO_2	dark	10	$<10^{-8}$	$<10^{-10}$ (dry; Knudsen cell reactor)	[2]

		85	$<10^{-8}$	$<10^{-9}$ (RH 25%; coated wall flow tube)	[3]
Al_2O_3	dark	7	3.2×10^{-8}	2×10^{-8} (dry; Knudsen cell reactor)	[4]
		80	1.4×10^{-8}	1.3×10^{-9}-2.6×10^{-8} (dry; DRIFTS)	[5]
NaCl	dark	5	$<10^{-8}$	$<10^{-4}$ (RH 75%; aerosol flow tube;)	[44]
		85	$<10^{-8}$	1×10^{-3}-3.7×10^{-4} (RH 50%-90%; aerosol flow tube;)	[45]
$CaCO_3$	dark	10	2.5×10^{-7}	$(4.25\pm1.18)\times10^{-9}$ (dry; DRIFTS) $(6.56\pm0.34)\times10^{-8}$ (wet; DRIFTS)	[6]
		32	1.8×10^{-7}		
		85	3.2×10^{-7}		
$(NH_4)_2SO_4$	dark	10	$<10^{-8}$	-	-
		56	$<10^{-8}$		
		85	$<10^{-8}$		
3.5 wt% NaCl solution	dark	-	1.4×10^{-8}	-	-
Bulk sea water	dark	-	1.6×10^{-8}	-	-
Urban grime	dark	5	$<10^{-7}$	-	-
		70	3.1×10^{-7}		
	irradiated	5	1.9×10^{-6}	$(1.1\pm0.2)\times10^{-6}$-$(5.8\pm0.7)\times10^{-6}$ (RH 0% - 90%; coated wall flow tube)	[33]
		70	5.8×10^{-6}		

3.2. NO_2 uptake on sea water

As discussed before, the sea surface was suggested to be a potential source of HONO [18], thus we used the wetted wall flow tube to investigate the NO_2 uptake on 3.5 wt% NaCl solution and sea water. Figure 3 shows the example result of the NO_2 uptake experiment on sea water. It was supervised to find that HONO production was observed in the flow tube system when NO_2 had not contacted with the sea water surface (step 1). The background HONO was probably produced on the wall of the path tubing. However, when the extractor was pulled down and the NO_2 contacted with the sea water, both concentrations of NO_2 and HONO decreased (step 2-4). And when the contact of the NO_2 with the sea water was stopped, the NO_2 and HONO concentrations returned back to the initial concentrations (step 5). The γ_{geo} of NO_2 on NaCl solution and sea water was then calculated to be 1.4×10^{-8} and 1.6×10^{-8}, respectively (Table 1). These results suggest that the NO_2 uptake on sea water might not be a significant pathway to release gaseous HONO, or the alkaline conditions of sea water could retain the formed acidic HONO in the aqueous phase. Our results cannot help explain the elevated NO_2-to-HONO conversion rate in the air masses passing by sea surfaces observed by Zha et al. [18]. Another possible reason could be that the sea water used in the present study was the bulk water, while at the air−sea interface, there is a sea-surface microlayer (SML) comprised of complex enriched organic matters [46,47], which might be able to promote the heterogeneous conversion of NO_2 to HONO. Further experiment with the sea-surface microlayer is needed to better understand the HONO formation on the sea surface.

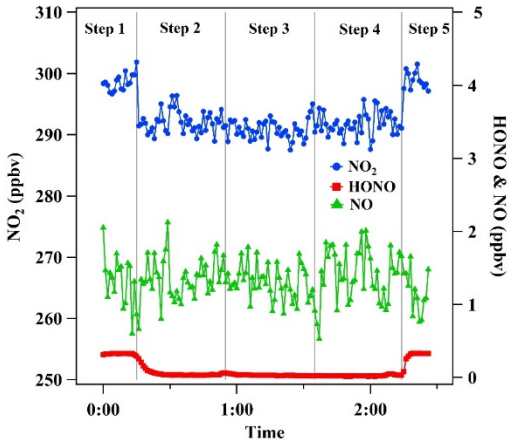

Figure 3. NO_2 uptake on bulk sea water. Blue circles, red squares and green triangles represent the NO_2, HONO and NO concentrations at the exit of the reactor. The grey vertical lines indicate the experimental steps. Step 1: the extractor was at top of the wetted wall flow tube, l = 0 cm; step 2: pulling down the extractor and the contact distance l = 10 cm; step 3: l = 20 cm; step 4: l = 30 cm; step 5: the extractor was pushed back to the top of the wetted wall flow tube, l = 0 cm.

3.3. NO_2 uptake on urban grime

Figure 4 shows the steps of one experimental cycle to determine NO_2 uptake on urban grime. First, NO_2 was not introduced into the box reactor but passed through a bypass line until the NO_2 initial concentration was stable (step 1). Then NO_2 was introduced into the box reactor with the UV-visible light off (step 2). When the concentration of HONO and NO_2 were stable, the light was turned on and NO_2 uptake remained constant as long as the light was on (step 3). After that, the light was turned off (step 4) and NO_2 was bypassed from the box reactor (step 5). When the urban grime was exposed to NO_2 in the dark condition, NO_2 concentration decreased slightly (step 2 and 4), corresponding to an uptake coefficient below 3.1×10^{-7}. When the light was turned on, there was an obvious decrease of NO_2 compared to dark condition, and the NO_2 uptake was constant during the irradiation (step 3). It suggests a weak uptake and reaction of NO_2 on urban grime in the dark condition, but an enhanced reaction under irradiation. The γ_{geo} on urban grime under irradiation was measured to be 1.9×10^{-6} at 5% RH and 5.8×10^{-6} at 70% RH, which shows a clear relative humidity dependence and is similar to the values of $(1.1\text{-}5.8)\times10^{-6}$ at RH 0% - 90% reported by Liu et al. [33].

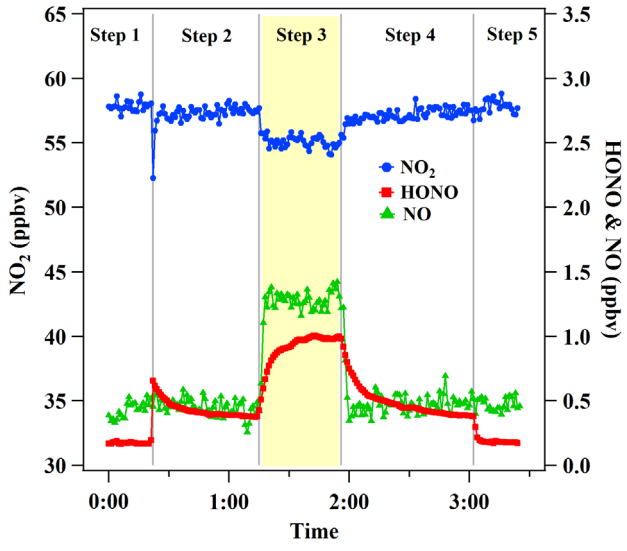

Figure 1. Conversion of NO_2 to HONO and NO on urban grime at 70% RH. Blue circles, red squares and green triangles represent the NO_2, HONO and NO concentrations at the exit of the reactor. The grey vertical lines indicate the experimental steps. Step 1: reactor bypass; step 2: urban grime exposed

to NO_2 in the dark; step 3: urban grime exposed to NO_2 under the irradiation; step 4: urban grime exposed to NO_2 in the dark; step 5: reactor bypass.

Photo-enhanced uptake of NO_2 has also been found on polycyclic aromatic hydrocarbons (PAHs) [7-10], soot [14,15] and mineral dust [3,16]. PAHs were proposed as photosensitizers to get excited under irradiation and react with NO_2, thus promote the NO_2 uptake [14]. Ndour et al. [16] found that TiO_2 can act as photocatalyst and enhance the reactivity of NO_2 on mineral dust under irradiation. The true uptake coefficient (γ_{BET}) measured on soot and mineral dust in previous studies was calculated by measuring BET surface area of particle samples, and thus it may not be comparable to the geometric uptake coefficient on urban grime in the present study. Nevertheless, the γ_{geo} values of $(1.8\pm0.3)\times10^{-6}$ on pyrene/KNO_3 under irradiation at 30-35% RH [9] are lower than the γ_{geo} on urban grime, which have more complex compositions than the proxies used in previous studies. In addition, Baltrusaitis et al. [48] found that NO_2 uptake was enhanced on α-Fe_2O_3 surface under UV irradiation with reduced nitrogen species found on the surface. Mineral species like Fe, which has been found in urban grime [30], along with mixture of PAHs, soot, TiO_2 and other photocatalysts in the urban grime, could significantly contribute to the photo-reactivity of urban grime and promote the NO_2-to-HONO conversion.

Formation of HONO and NO were also observed from the NO_2 uptake reactions on urban grime. When urban grime was exposed to NO_2 in the dark condition (cf. step 2 and step 4 in Figure 4), the heterogeneous reaction of NO_2 only produced ~0.22 ppbv of HONO. At step 3, when urban grime was exposed to NO_2 under irradiation, enhanced formations of HONO (~0.86 ppbv) and NO (0.79 ppbv) were both observed. Nanayakkara et. al. [22] has shown that the photolysis of nitrate can contribute to HONO formation, so a photolysis experiment without NO_2 input was also carried out in the present study to assess the contribution from nitrate. Photolysis of nitrate in urban grime only contributed to ~0.20 ppbv of HONO, and there was no NO formation during the photolysis experiment, which indicated that NO formation was not due to the photolysis of HONO (figure not shown here). Furthermore, based on the measured photolysis frequency of NO_2 (j_{NO2}, 1.8×10^{-4} s^{-1}), the photolysis only contributed to a loss of 0.7% of the total NO_2, suggesting that the formation of NO via NO_2 photolysis was also neglected in the present study. Similar to the present study, both formations of HONO and NO have been observed on illuminated PAHs and soot, and were attributed to the photosensitized reactions of NO_2 with PAHs [7-10,14]. The observed HONO and NO could be contributed from the photo-reduction of NO_2 with PAHs or soot in urban grime. However, only HONO formation was observed during the illuminated uptake of NO_2 on urban grime collected in Guangzhou [33], which may suggest the different reactions undergo on the surface of urban grime with different compositions. More experiments under different conditions with urban grime collected from different locations are still needed to better understand the NO_2 uptake and reactions on urban grime. Furthermore, the inorganic ions in the reacted and fresh urban grime was also compared in the present study (Figure 5), and the mass fraction of nitrate in urban grime increased after exposure to NO_2 under irradiation. This indicated that the heterogeneous NO_2 uptake on urban grime also produced particulate nitrate besides the reduced gas phase products.

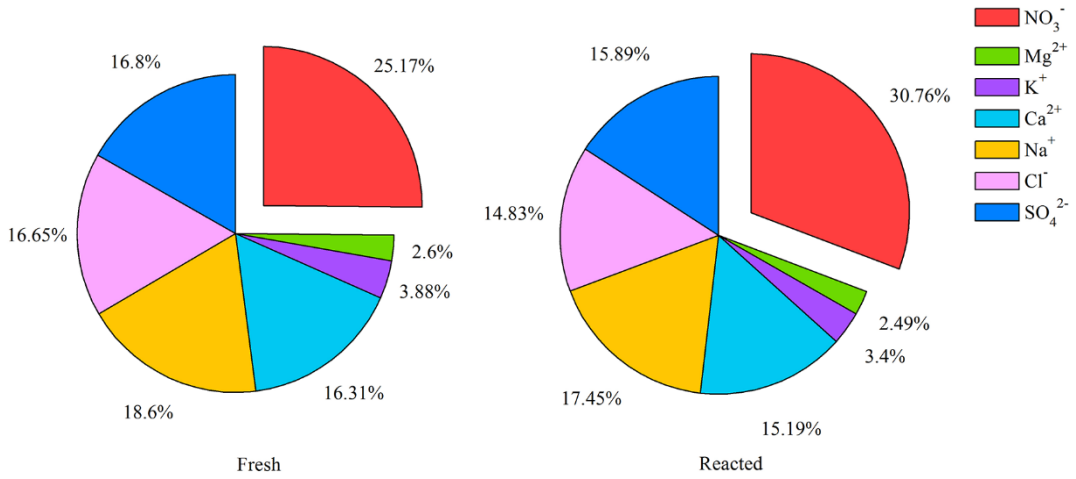

Figure 5. Mass fractions of inorganic ions in the fresh urban grime and in the reacted urban grime after the irradiation experiment.

The yields of NO and HONO on urban grime were calculated from the ratio of the net formation of NO or HONO to the net consumption of NO_2 by Eq.5. The HONO yield was estimated to be 28% at 5% RH and 46% at 70% RH, and the NO yield was estimated to be 16% at 5% RH and 11% at 70% RH under irradiation. The positive correlations of NO_2 uptake and HONO formation with RH, indicating that high RH could enhance the uptake reaction. The amount of the absorbed water on urban grime has been found positively related with RH [23]. The absorbed water could enhance the uptake by increasing the mobility of reagents [50] or reducing the viscosity of the surface [51]. Such changes in mobility of reagents and viscosity of the surface could promote the reaction of NO_2 and the release of volatile products.

3.4. Atmospheric implication on HONO unknown source

The photo-enhanced HONO formation via NO_2 uptake could influence the oxidation capacity of the urban atmosphere, as an important source of OH radical (e.g. [52]). The flux of HONO production under irradiation can be calculated from the experiments, and it was determined to be 1.9×10^9 molecules cm^{-2} s^{-1} at 5% RH and 5.3×10^9 molecules cm^{-2} s^{-1} at 70% RH. Given in an urban area with 57 ppbv of NO_2 in a 10 m width street and 20 m height building covered with urban grime, an estimation of HONO source strength from urban grime could give 0.25 ppbv h^{-1} at 5% RH and 0.71 ppbv h^{-1} at 70% RH. Tang et al. [53] found that there was high daytime missing sources of HONO in Beijing-Tianjin-Heibei region in China and the missing sources reached a maximum of 2.5 ppbv h^{-1}. Lee et al. [54] also reported the daytime missing source of HONO maximum of ~2.8 ppbv h^{-1} in London. Accordingly, in highly urbanized area, urban surfaces covered by urban grime such as buildings and roads provide a large surface area and the NO_2 uptake on the urban grime could be an important source of HONO in daytime, and should be considered in the simulation of HONO levels in future modeling studies.

In view of the unknown HONO sources observed in different places, many air quality models have incorporated the NO_2 uptake process to better simulating the atmospheric HONO loading, which is of vital importance in assessing the oxidation capacity of the lower troposphere in polluted regions. In some model studies, larger γ were applied to better match the simulated HONO levels to measurements (e.g. [28,55,56]). Nighttime uptake coefficients of 5×10^{-6} and 1×10^{-5} on aerosol surface were used by Zhang et al. [55] and Zhang et al. [56], respectively, following the model setup in Li et al. [57]. Yet, the uptake coefficient in Li et al. [57] was set as 1×10^{-6} according to a laboratory experiment for the NO_2 uptake on pure water and acidic solution [58]. Zhang et al. [28] adopted a large uptake coefficient of 2×10^{-5} on aerosol surface when sunlight was available, while the uptake coefficients reported by the references there ranged from 1.2×10^{-7} to 6×10^{-6} [7,11,14,16]. The CAMQ model adopted the γ_{geo} of 1×10^{-6} measured on tunnel wall by Kurtenbach et al. [20] to simulate the

heterogeneous formation of HONO on urban, leaves, and particle surfaces [59-61]. However, the real surface of the porous residue on the tunnel wall was not taken into consideration in γ_{geo}, and thus the true uptake coefficient on the residue particles should be smaller than the measured γ_{geo} [20], which should be only suitable for geometric surfaces such as ground and building surfaces. Besides, several model studies also used the γ_{geo} measured by Kurtenbach et al. [20] as the γ_{BET} on particles [62-64]. Instead, the true uptake coefficient on particles such as γ_{BET} or γ measured in aerosol flow tube with directly measured particle surface area should be used in such cases. Inappropriate usages of γ of NO_2 in air quality models could lead to misestimates of HONO. Therefore, more direct measurement of γ of NO_2 with real ambient aerosol and urban grime with mixture composition are needed. The uptake of NO_2 on different surfaces with different γ values also should be separately treated in the air quality models.

4. Conclusions

Heterogeneous uptake of NO_2 on different surfaces is an important process in controlling the NO_x removal from the atmosphere, and accurate representation of the NO_2 uptake coefficient in air quality models is of paramount importance for predicting the atmospheric NO_x cycling and photochemistry. In the present study, we measured the NO_2 uptake on different surfaces, including inorganic particles, sea water and urban grime, using three different flow tube reactors. The reactivity of NO_2 was found very weak in dark condition on such surfaces. But UV-visible illumination enhanced the NO_2 uptake on urban grime by two orders of magnitude. HONO and NO formations were observed from the photo-enhanced NO_2 uptake on urban grime. The flux of HONO production from irradiated urban grime was determined to be $1.9\text{-}5.3\times10^{9}$ molecules cm^{-2} s^{-1} at RH of 5% to 70%, which could lead to a daytime HONO source of 0.25-0.71 ppbv h^{-1} in a presumptive urban street. The photo-enhanced NO_2 uptake on urban grime could increase the daytime HONO levels in the polluted urban atmosphere, and should be considered in future experimental and modeling studies.

Author Contributions: Conceptualization, T.W., C.G., Z.W. and C.Y.; methodology, T.W., C.G., Z.W. and C.Y.; validation, X.X., Y.Y. and Z.Z.; formal analysis, C.Y. and Q.M.; resources, T.W.; data curation, X.X.; writing—original draft preparation, C.Y.; writing—review and editing, T.W., Z.W., Q.M., C.G., and C.Y.; supervision, T.W.; project administration, T.W. and C.G. ; funding acquisition, T.W. All authors have read and agreed to the published version of the manuscript.

Funding: This study is funded by the National Natural Science Foundation of China, (91544213, 91744204) and the Research Grants Council of Hong Kong Special Administrative Region, China (T24/504/17, C5022-14G, 15265516) and ANR-RGC Joint Research Scheme (project A-PolyU502/16 - SEAM).

Acknowledgments: We thank Dr. Tommy Wei for his help in the measurement of spectral irradiance of the UV-visible light.

Conflicts of Interest: The authors declare no conflict of interest.

References

1. Finlayson-Pitts, B.J.; Wingen, L.M.; Sumner, A.L.; Syomin, D.; Ramazan, K.A. The heterogeneous hydrolysis of NO_2 in laboratory systems and in outdoor and indoor atmospheres: An integrated mechanism. *Physical Chemistry Chemical Physics* **2003**, *5*, 223-242.
2. Underwood, G.M.; Song, C.H.; Phadnis, M.; Carmichael, G.R.; Grassian, V.H. Heterogeneous reactions of NO_2 and HNO_3 on oxides and mineral dust: A combined laboratory and modeling study. *Journal of Geophysical Research: Atmospheres* **2001**, *106*, 18055-18066.
3. Ndour, M.; Nicolas, M.; D'Anna, B.; Ka, O.; George, C. Photoreactivity of NO_2 on mineral dusts originating from different locations of the sahara desert. *Physical chemistry chemical physics : PCCP* **2009**, *11*, 1312-1319.
4. Underwood, G.; Miller, T.; Grassian, V. Transmission FT-IR and Knudsen cell study of the heterogeneous reactivity of gaseous nitrogen dioxide on mineral oxide particles. *The Journal of Physical Chemistry A* **1999**, *103*, 6184-6190.
5. Börensen, C.; Kirchner, U.; Scheer, V.; Vogt, R.; Zellner, R. Mechanism and kinetics of the reactions of NO_2 or HNO_3 with alumina as a mineral dust model compound. *The Journal of Physical Chemistry A* **2000**, *104*, 5036-5045.

6. Li, H.J.; Zhu, T.; Zhao, D.F.; Zhang, Z.F.; Chen, Z.M. Kinetics and mechanisms of heterogeneous reaction of NO_2 on $CaCO_3$ surfaces under dry and wet conditions. *Atmos. Chem. Phys.* **2010**, *10*, 463-474.
7. George, C.; Strekowski, R.S.; Kleffmann, J.; Stemmler, K.; Ammann, M. Photoenhanced uptake of gaseous NO_2 on solid-organic compounds: A photochemical source of HONO? *Faraday Discussions* **2005**, *130*, 195-210.
8. Brigante, M.; Cazoir, D.; D'Anna, B.; George, C.; Donaldson, D.J. Photoenhanced uptake of NO_2 by pyrene solid films. *The Journal of Physical Chemistry A* **2008**, *112*, 9503-9508.
9. Ammar, R.; Monge, M.E.; George, C.; D'Anna, B. Photoenhanced NO_2 loss on simulated urban grime. *Chemphyschem : a European journal of chemical physics and physical chemistry* **2010**, *11*, 3956-3961.
10. Cazoir, D.; Brigante, M.; Ammar, R.; D'Anna, B.; George, C. Heterogeneous photochemistry of gaseous NO_2 on solid fluoranthene films: A source of gaseous nitrous acid (HONO) in the urban environment. *Journal of Photochemistry and Photobiology A: Chemistry* **2014**, *273*, 23-28.
11. Stemmler, K.; Ammann, M.; Donders, C.; Kleffmann, J.; George, C. Photosensitized reduction of nitrogen dioxide on humic acid as a source of nitrous acid. *Nature* **2006**, *440*, 195-198.
12. Stemmler, K.; Ndour, M.; Elshorbany, Y.; Kleffmann, J.; D'anna, B.; George, C.; Bohn, B.; Ammann, M. Light induced conversion of nitrogen dioxide into nitrous acid on submicron humic acid aerosol. *Atmospheric Chemistry and Physics* **2007**, *7*, 4237-4248.
13. Han, C.; Yang, W.; Wu, Q.; Yang, H.; Xue, X. Heterogeneous photochemical conversion of NO_2 to HONO on the humic acid surface under simulated sunlight. *Environmental science & technology* **2016**, *50*, 5017-5023.
14. Monge, M.E.; D'Anna, B.; Mazri, L.; Giroir-Fendler, A.; Ammann, M.; Donaldson, D.J.; George, C. Light changes the atmospheric reactivity of soot. *Proceedings of the National Academy of Sciences of the United States of America* **2010**, *107*, 6605-6609.
15. Guan, C.; Li, X.; Zhang, W.; Huang, Z. Identification of nitration products during heterogeneous reaction of NO_2 on soot in the dark and under simulated sunlight. *The journal of physical chemistry. A* **2017**, *121*, 482-492.
16. Ndour, M.; D'Anna, B.; George, C.; Ka, O.; Balkanski, Y.; Kleffmann, J.; Stemmler, K.; Ammann, M. Photoenhanced uptake of NO_2 on mineral dust: Laboratory experiments and model simulations. *Geophysical Research Letters* **2008**, *35*.
17. Kleffmann, J. Daytime sources of nitrous acid (HONO) in the atmospheric boundary layer. *Chemphyschem : a European journal of chemical physics and physical chemistry* **2007**, *8*, 1137-1144.
18. Zha, Q.; Xue, L.; Wang, T.; Xu, Z.; Yeung, C.; Louie, P.K.K.; Luk, C.W.Y. Large conversion rates of NO_2 to HNO_2 observed in air masses from the south china sea: Evidence of strong production at sea surface? *Geophysical Research Letters* **2014**, *41*, 7710-7715.
19. Su, H.; Cheng, Y.; Oswald, R.; Behrendt, T.; Trebs, I.; Meixner, F.X.; Andreae, M.O.; Cheng, P.; Zhang, Y.; Poschl, U. Soil nitrite as a source of atmospheric HONO and OH radicals. *Science* **2011**, *333*, 1616-1618.
20. Kurtenbach, R.; Becker, K.H.; Gomes, J.A.G.; Kleffmann, J.; Lorzer, J.C.; Spittler, M.; Wiesen, P.; Ackermann, R.; Geyer, A.; Platt, U. Investigations of emissions and heterogeneous formation of HONO in a road traffic tunnel. *Atmospheric Environment* **2001**, *35*, 3385-3394.
21. Liang, Y.; Zha, Q.; Wang, W.; Cui, L.; Lui, K.H.; Ho, K.F.; Wang, Z.; Lee, S.-c.; Wang, T. Revisiting nitrous acid (HONO) emission from on-road vehicles: A tunnel study with a mixed fleet. *Journal of the Air & Waste Management Association* **2017**, *67*, 797-805.
22. Nanayakkara, C.E.; Jayaweera, P.M.; Rubasinghege, G.; Baltrusaitis, J.; Grassian, V.H. Surface photochemistry of adsorbed nitrate: The role of adsorbed water in the formation of reduced nitrogen species on alpha-Fe_2O_3 particle surfaces. *The journal of physical chemistry. A* **2014**, *118*, 158-166.
23. Baergen, A.M.; Donaldson, D.J. Photochemical renoxification of nitric acid on real urban grime. *Environmental science & technology* **2013**, *47*, 815-820.
24. Ye, C.; Gao, H.; Zhang, N.; Zhou, X. Photolysis of nitric acid and nitrate on natural and artificial surfaces. *Environmental science & technology* **2016**, *50*, 3530-3536.
25. Ye, C.; Zhang, N.; Gao, H.; Zhou, X. Photolysis of particulate nitrate as a source of HONO and NO_x. *Environmental science & technology* **2017**, *51*, 6849-6856.
26. Zhou, X.; Gao, H.; He, Y.; Huang, G.; Bertman, S.B.; Civerolo, K.; Schwab, J. Nitric acid photolysis on surfaces in low-NO_x environments: Significant atmospheric implications. *Geophysical research letters* **2003**, *30*.

27. Laufs, S.; Kleffmann, J. Investigations on HONO formation from photolysis of adsorbed HNO_3 on quartz glass surfaces. *Physical chemistry chemical physics : PCCP* **2016**, *18*, 9616-9625.
28. Zhang, L.; Wang, T.; Zhang, Q.; Zheng, J.; Xu, Z.; Lv, M. Potential sources of nitrous acid (HONO) and their impacts on ozone: A WRF-Chem study in a polluted subtropical region. *Journal of Geophysical Research: Atmospheres* **2016**, *121*, 3645-3662.
29. Baergen, A.M.; Styler, S.A.; van Pinxteren, D.; Muller, K.; Herrmann, H.; Donaldson, D.J. Chemistry of urban grime: Inorganic ion composition of grime vs particles in Leipzig, Germany. *Environmental science & technology* **2015**, *49*, 12688-12696.
30. Lam, B.; Diamond, M.L.; Simpson, A.J.; Makar, P.A.; Truong, J.; Hernandez-Martinez, N.A. Chemical composition of surface films on glass windows and implications for atmospheric chemistry. *Atmospheric Environment* **2005**, *39*, 6578-6586.
31. Butt, C.M.; Diamond, M.L.; Truong, J.; Ikonomou, M.G.; Ter Schure, A.F. Spatial distribution of polybrominated diphenyl ethers in southern Ontario as measured in indoor and outdoor window organic films. *Environmental science & technology* **2004**, *38*, 724-731.
32. Liu, Q.-T.; Chen, R.; McCarry, B.E.; Diamond, M.L.; Bahavar, B. Characterization of polar organic compounds in the organic film on indoor and outdoor glass windows. *Environmental science & technology* **2003**, *37*, 2340-2349.
33. Liu, J.; Li, S.; Mekic, M.; Jiang, H.; Zhou, W.; Loisel, G.; Song, W.; Wang, X.; Gligorovski, S. Photoenhanced uptake of NO_2 and HONO formation on real urban grime. *Environmental Science & Technology Letters* **2019**.
34. Han, C.; Liu, Y.; He, H. Role of organic carbon in heterogeneous reaction of NO_2 with soot. *Environmental science & technology* **2013**, *47*, 3174-3181.
35. Liu, Y.; Han, C.; Ma, J.; Bao, X.; He, H. Influence of relative humidity on heterogeneous kinetics of NO_2 on kaolin and hematite. *Physical chemistry chemical physics : PCCP* **2015**, *17*, 19424-19431.
36. Ma, Q.; Wang, T.; Liu, C.; He, H.; Wang, Z.; Wang, W.; Liang, Y. SO_2 initiates the efficient conversion of NO_2 to HONO on MgO surface. *Environmental science & technology* **2017**, *51*, 3767-3775.
37. Behnke, W.; George, C.; Scheer, V.; Zetzsch, C. Production and decay of $ClNO_2$ from the reaction of gaseous N_2O_5 with NaCl solution: Bulk and aerosol experiments. *Journal of Geophysical Research: Atmospheres* **1997**, *102*, 3795-3804.
38. Gutzwiller, L.; Arens, F.; Baltensperger, U.; Gaggeler, H.W.; Ammann, M. Significance of semivolatile diesel exhaust organics for secondary HONO formation. *Environmental science & technology* **2002**, *36*, 677-682.
39. Heland, J.; Kleffmann, J.; Kurtenbach, R.; Wiesen, P. A new instrument to measure gaseous nitrous acid (HONO) in the atmosphere. *Environmental science & technology* **2001**, *35*, 3207-3212.
40. Xu, Z.; Wang, T.; Wu, J.; Xue, L.; Chan, J.; Zha, Q.; Zhou, S.; Louie, P.K.K.; Luk, C.W.Y. Nitrous acid (HONO) in a polluted subtropical atmosphere: Seasonal variability, direct vehicle emissions and heterogeneous production at ground surface. *Atmospheric Environment* **2015**, *106*, 100-109.
41. Cooney, D.O.; Kim, S.-S.; Davis, E.J. Analyses of mass transfer in hemodialyzers for laminar blood flow and homogeneous dialysate. *Chemical Engineering Science* **1974**, *29*, 1731-1738.
42. Murphy, D.M.; Fahey, D.W. Mathematical treatment of the wall loss of a trace species in denuder and catalytic converter tubes. *Analytical Chemistry* **1987**, *59*, 2753-2759.
43. Underwood, G.; Li, P.; Usher, C.; Grassian, V. Determining accurate kinetic parameters of potentially important heterogeneous atmospheric reactions on solid particle surfaces with a Knudsen cell reactor. *The Journal of Physical Chemistry A* **2000**, *104*, 819-829.
44. Abbatt, J.; Waschewsky, G. Heterogeneous interactions of HOBr, HNO_3, O_3, and NO_2 with deliquescent NaCl aerosols at room temperature. *The Journal of Physical Chemistry A* **1998**, *102*, 3719-3725.
45. Harrison, R.M.; Collins, G.M. Measurements of reaction coefficients of NO_2 and HONO on aerosol particles. *Journal Of Atmospheric Chemistry* **1998**, *30*, 397-406.
46. Donaldson, D.J.; George, C. Sea-surface chemistry and its impact on the marine boundary layer. *Environmental science & technology* **2012**, *46*, 10385-10389.
47. Wurl, O.; Obbard, J.P. A review of pollutants in the sea-surface microlayer (SML): A unique habitat for marine organisms. *Marine pollution bulletin* **2004**, *48*, 1016-1030.
48. Baltrusaitis, J.; Jayaweera, P.M.; Grassian, V.H. XPS study of nitrogen dioxide adsorption on metal oxide particle surfaces under different environmental conditions. *Physical Chemistry Chemical Physics* **2009**, *11*, 8295-8305.

49. Baergen, A.M.; Donaldson, D.J. Photochemical renoxification of nitric acid on real urban grime. *Environmental science & technology* **2013**, *47*, 815-820.
50. Rubasinghege, G.; Grassian, V.H. Role(s) of adsorbed water in the surface chemistry of environmental interfaces. *Chemical communications (Cambridge, England)* **2013**, *49*, 3071-3394.
51. Renbaum-Wolff, L.; Grayson, J.W.; Bateman, A.P.; Kuwata, M.; Sellier, M.; Murray, B.J.; Shilling, J.E.; Martin, S.T.; Bertram, A.K. Viscosity of α-pinene secondary organic material and implications for particle growth and reactivity. *Proceedings of the National Academy of Sciences - PNAS* **2013**, *110*, 8014-8019.
52. Elshorbany, Y.F.; Kurtenbach, R.; Wiesen, P.; Lissi, E.; Rubio, M.; Villena, G.; Gramsch, E.; Rickard, A.R.; Pilling, M.J.; Kleffmann, J. Oxidation capacity of the city air of Santiago, Chile. *Atmospheric Chemistry And Physics* **2009**, *9*, 2257-2273.
53. Tang, Y.; An, J.; Wang, F.; Li, Y.; Qu, Y.; Chen, Y.; Lin, J. Impacts of an unknown daytime HONO source on the mixing ratio and budget of hono, and hydroxyl, hydroperoxyl, and organic peroxy radicals, in the coastal regions of china. *Atmospheric Chemistry and Physics* **2015**, *15*, 9381-9398.
54. Lee, J.D.; Whalley, L.K.; Heard, D.E.; Stone, D.; Dunmore, R.E.; Hamilton, J.F.; Young, D.E.; Allan, J.D.; Laufs, S.; Kleffmann, J. Detailed budget analysis of HONO in central London reveals a missing daytime source. *Atmos. Chem. Phys.* **2016**, *16*, 2747-2764.
55. Zhang, J.; An, J.; Qu, Y.; Liu, X.; Chen, Y. Impacts of potential HONO sources on the concentrations of oxidants and secondary organic aerosols in the Beijing-Tianjin-Hebei region of china. *The Science of the total environment* **2019**, *647*, 836-852.
56. Zhang, J.; Guo, Y.; Qu, Y.; Chen, Y.; Yu, R.; Xue, C.; Yang, R.; Zhang, Q.; Liu, X.; Mu, Y., *et al.* Effect of potential HONO sources on peroxyacetyl nitrate (PAN) formation in eastern china in winter. *Journal of environmental sciences (China)* **2020**, *94*, 81-87.
57. Li, G.; Lei, W.; Zavala, M.; Volkamer, R.; Dusanter, S.; Stevens, P.; Molina, L.T. Impacts of HONO sources on the photochemistry in Mexico City during the MCMA-2006/MILAGO Campaign. *Atmospheric chemistry and physics* **2010**, *10*, 6551-6567.
58. Kleffmann, J.; Becker, K.H.; Wiesen, P. Heterogeneous NO_2 conversion processes on acid surfaces: Possible atmospheric implications. *Atmospheric Environment* **1998**, *32*, 2721-2729.
59. 1. Binkowski, F.S.; Roselle, S.J. Models-3 Community Multiscale Air Quality (cmaq) model aerosol component 1. Model description. *Journal of Geophysical Research D: Atmospheres* **2003**, *108*.
60. Byun, D.; Schere, K.L. Review of the governing equations, computational algorithms, and other components of the Models-3 Community Multiscale Air Quality (CMAQ) modeling system. *Applied mechanics reviews* **2006**, *59*, 51-76.
61. Foley, K.M.; Roselle, S.J.; Appel, K.W.; Bhave, P.V.; Pleim, J.E.; Otte, T.L.; Mathur, R.; Sarwar, G.; Young, J.O.; Gilliam, R.C., *et al.* Incremental testing of the Community Multiscale Air Quality (CMAQ) modeling system version 4.7. *Geoscientific model development* **2010**, *3*, 205-226.
62. Vogel, B.; Vogel, H.; Kleffmann, J.; Kurtenbach, R. Measured and simulated vertical profiles of nitrous acid—part II. Model simulations and indications for a photolytic source. *Atmospheric Environment* **2003**, *37*, 2957-2966.
63. Sarwar, G.; Roselle, S.J.; Mathur, R.; Appel, W.; Dennis, R.L.; Vogel, B. A comparison of CMAQ HONO predictions with observations from the Northeast Oxidant And Particle Study. *Atmospheric environment (1994)* **2008**, *42*, 5760-5770.
64. Czader, B.H.; Rappenglück, B.; Percell, P.; Byun, D.W.; Ngan, F.; Kim, S. Modeling nitrous acid and its impact on ozone and hydroxyl radical during the Texas Air Quality Study 2006. *Atmospheric chemistry and physics* **2012**, *12*, 6939-6951.